Orbital Picture in Molecular Inner-Shell Excited States of Rydberg-Valence Mixed Character

Nobuhiro Kosugi
UVSOR, Institute for Molecular Science, Myodaiji, Okazaki 444-8585, Japan

Received on 14 January, 2005

The core-to-σ* excited state is repulsive for the bond elongation; on the other hand, the core ionized state and the core-to-π* state are bound and the core-to-Rydberg states are almost parallel to the potential energy curve of the core ionized state. Thus, the core-electron excitation to the unoccupied σ* orbital can be mixed with the one-electron Rydberg or continuum orbital, as dependent on the bond distance, and even with the unoccupied π* orbital in some cases. Within the framework of one-electron picture, we show σ* orbitals mixed with Rydberg character in the 1s excitation of O_2 and CH_3F, and Rydberg orbitals mixed with valence character in the 1s excitation of CH_4, CO_2, and N_2O.

I. INTRODUCTION

The atomic and molecular core-to-Rydberg excitation is converging to a certain core ionization threshold (E_{th}). In addition, most molecules have unoccupied molecular orbitals of anti-bonding valence character such as σ* and π*. These anti-bonding orbitals can also accept an excited electron from the inner shell. The potential energy curve of the core-to-σ* valence excited state [1] is repulsive for a specified σ bond; then, the core-to-σ* excited state is lower than the continuum and Rydberg region at the longer bond distance and is embedded in the continuum at the shorter distance. That is, two kinds of interaction involving the valence state should be discussed along the potential energy curve for a specified σ bond[1]: the Rydberg-valence interaction below E_{th} and the continuum-valence interaction above E_{th}. In the present work, we discuss the former interaction within one-electron picture and show how the valence and/or Rydberg orbitals look like through the interactions.

II. RYDBERG CONTRIBUTION IN CORE-TO-σ* EXCITATION

A. O_2

N_2 has a triple covalent bond and the $3\sigma_u$* molecular orbital is of strong antibonding character; then, the N1s excitation to this σ* orbital is observed above E_{th} as a well-known shape resonance. In molecules having weak covalent bonds, the 1s→ σ* excited state is possibly observed below E_{th}. We can expect Rydberg-valence (RV) mixings in the case of the same p-symmetry as the 2pσ* orbital. As already discussed [1,2], the strong RV mixing results in new potential energy curves due to the avoided curve crossing of the Rydberg (p-type) and valence (2pσ*) states.

The Rydberg features in the O 1s excitation spectrum of O_2 with a triplet ground state ($^3\Sigma_g^+$) are very complicated due to two ionization thresholds, $^4\Sigma^+$ and $^2\Sigma^+$ [2,3]. The angle-resolved photoion spectroscopy (ARPIS) has shown that the core-to-σ* ($3\sigma_u$*) excited states give exchange-split two strong resonances in the Rydberg region [2,3] and that the $^4\Sigma^+$ channel gives vibrational enhancements in the 3pσ Rydberg state and the $^2\Sigma^+$ channel has no distinct evidence for the RV mixing [2]. Fig. 1 shows (a) this $3\sigma_u$* orbital before the RV mixing and (b) the RV-mixed 3pσ-$3\sigma_u$* orbital in the Franck-Condon region. This kind of the RV mixing is not effective for the s-type or d-type Rydberg states with different symmetry from the 2pσ* orbital.

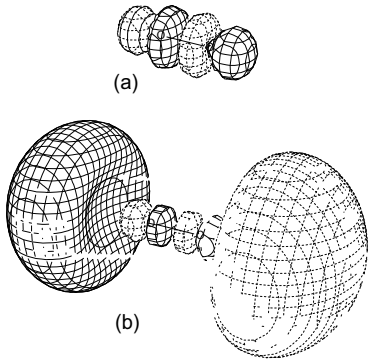

FIG. 1: Contour maps of (a) the $3\sigma_u$* orbital obtained before the RV mixing (without any diffuse function) and (b) the RV-mixed 3pσ-$3\sigma_u$* orbital in the O1s excitation of O_2.

B. CH_3 F

In N_2, the N1s excitation to the π* orbital is located lower than the Rydberg region. Even in saturated molecules, the excitation to the σ* orbital is possibly located below the Rydberg region in the case of very weak σ covalent bonds. In CH_3F with a very weak σ covalent bond between CH_3 and F, we have observed a broad and strong σ* ($6a_1$) band below the Rydberg region and a weak shoulder arising from the $3sa_1$ Rydberg [4]. The σ* ($6a_1$) and $3sa_1$ Rydberg orbitals are shown in Fig. 2, indicating that the $3sa_1$ orbital of the CH_3 fragment is deformed by orthogonalization to the valence electrons of the F atom. There might be more or less RV mixing due to the avoided crossing for the same a_1 symmetry.

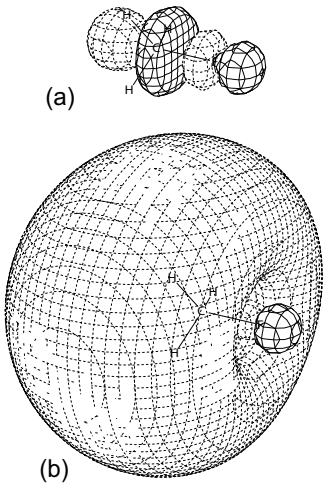

FIG. 2: Contour maps of (a) the σ* ($6a_1$*) orbital and (b) the $3sa_1$ Rydberg orbital in the C1s excitation of CH_3F.

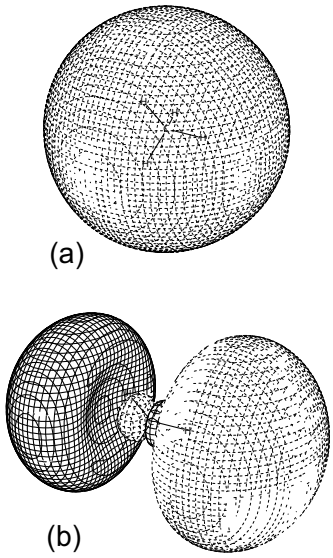

FIG. 3: Contour maps of (a) the $3sa_1$ Rydberg orbital and (b) one of the three $3pt_2$ Rydberg orbitals in the C1s excitation of CH_4. The $3pt_2$orbital has no valence contribution and is purely atomic-like.

III. VALENCE CONTRIBUTION IN CORE-TO-RYDBERG EXCITATION

A. CH_4

A simple molecular orbital picture predicts that the CH_4 molecule has the $2t_2$* and $3a_1$* antibonding molecular orbitals. In the case of inner-shell excitation, the C1s $(1a_1) \rightarrow 3a_1$ excitation is dipole forbidden but the C1s $(1a_1) \rightarrow 2t_2$ excitation is dipole allowed. However, no distinct $2t_2$* resonance is observed in the C1s photoabsorption of CH_4[5]. The C1s photoabsorption spectrum shows many distinct Rydberg states, vibronically allowed $3sa_1$, strong npt_2 series, and ndt_2 series. The Rydberg region in CH_4 (C1s) [5] seems to be almost the same as in CH_3F (C1s) [4]. It is noticed that the C1s $(1a_1) \rightarrow 3pt_2$ Rydberg excited state with three-fold degeneracy should be affected by Jahn-Teller (JT) distortion. Fig. 3 shows one of the three degenerate $3pt_2$ Rydberg orbitals in CH_4 in comparison with the $3sa_1$ Rydberg orbital. Considering that the $3pt_2$ orbital has no valence contribution and is purely atomic-like, we could expect a very weak JT distortion in the $3pt_2$ Rydberg state [6]. However, recent high-resolution C1s photoabsorption spectra of CH_4 [7,8] have shown that the $3pt_2$ Rydberg state shows strong vibrational contributions in addition to the total symmetric vibration. This vibrational enhancement should arise from the JT effect in CH_4. Fig. 4 shows (b) a C_{3v}-distorted 3p Rydberg orbital, together with (a) the $2t_2$* orbital obtained without any diffuse function. The JT distorted $3pt_2$ orbital can get a large $2t_2$* contribution. This valence mixing gives intensities to the vibronically excited states of the C1s $(1a_1) \rightarrow 3pt_2$ excitation.

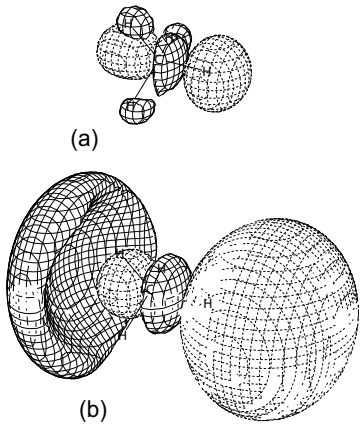

FIG. 4: Contour maps of (a) the $2t_2$* orbital obtained without any diffuse function and (b) a C_{3v}-distorted "$3pt_2$" orbital in the C1s excitation of CH_4. The $2t_2$* valence mixing gives intensities to the vibronically excited states of the C1s $(1a_1) \rightarrow 3pt_2$ excitation.

B. CO_2(C1s)

In the C1s $(2\sigma_g)$ excitation spectrum of CO_2, the strongest Rydberg state is of $3s\sigma_g$ symmetry [8,9]. However, the C1s $(2\sigma_g) \rightarrow 3s\sigma_g$ Rydberg excitation is dipole-forbidden. Fig. 5 shows a contour map of the $3s\sigma_g$ Rydberg orbital (Fig. 5(a)), which is mixed with the $5\sigma_g$* antibonding orbital (Fig. 5(b)). This valence mixing does not give any intensity from the C1s $(2\sigma_g)$. On the other hand, Fig. 6 shows an orbital map for the same 3s Rydberg orbital at a bent geometry. The 3s Rydberg state has a large π* contribution. The C1s $(2\sigma_g) \rightarrow 2\pi_u$* valence excited state has a stable bent geometry due to the Renner-Teller effect on electronically degenerate states in linear polyatomic systems [10]. This bending geometry, or bend-

ing motion in terms of molecular dynamics, is related to the vibronically induced $3s\sigma_g$ Rydberg transition. In high-resolution ARPIS spectra, bending vibrational fine structures are resolved in the C1s $(2\sigma_g) \rightarrow 3s\sigma_g$ and $4s\sigma_g$ Rydberg bands [8,9].

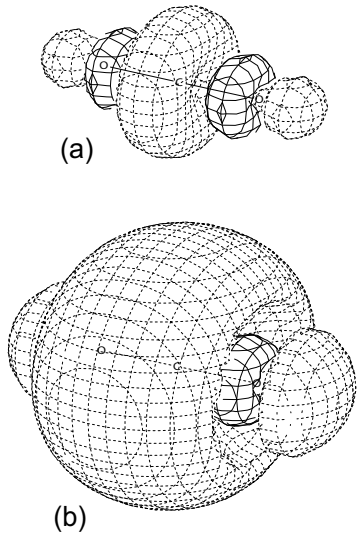

FIG. 5: Contour maps of (a) the $5\sigma_g$* valence orbital obtained without any diffuse function and (b) the $3s\sigma_g$ Rydberg orbital in the C1s $(2\sigma_g)$ excitation of CO_2.

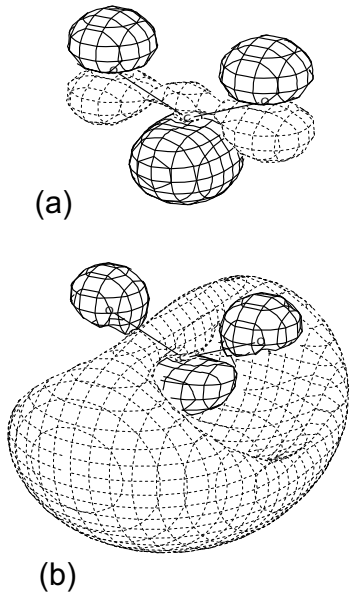

FIG. 6: Contour maps of (a) the π* orbital and (b) the 3s Rydberg orbital at a bent geometry in the C1s excitation of CO_2. The 3s Rydberg orbital has a large π* valence contribution.

C. N_2O and CO_2 (terminal N and O)

N_2O and CO_2 are isoelectronic and the molecular orbitals look similar. The lowest σ* (8σ*) and 3s Rydberg orbitals excited from the central N (N_c) are shown in Fig. 7. The orbital character is nearly the same as in CO_2(C1s) shown in Fig. 5. The N_c 1s excitation of N_2O is expected to be similar to the C1s excitation of CO_2. Unfortunately, the N1s excitation spectra include contributions from two N 1s edges and do not show clear evidence for bending mode coupling in the N_c manifold [11]. On the other hand, the lowest σ* orbitals (8σ* of N_2O in Fig. 7(a) and $5\sigma_g$* of CO_2in Fig. 5(a)) have a large pσ component on the terminal N (N_t) and O. Fig. 8 shows a contour map of the "4s" Rydberg orbital excited from the N_t 1s. The N_t 4s Rydberg orbital has a large 8σ* contribution with a pσ component as shown in Fig. 7(a) and get its intensity from the N_t 1s$\rightarrow$pσ component [1,11]. Although the s-type Rydberg series is generally expected to be weak in the 1s photoabsorption, the Rydberg regions of the N_t 1s and O1s excitations of N_2O and CO_2 are dominated in the observed spectra [7,8,11] by the s-type Rydberg states (4s most dominant) due to the lowest σ* mixing with the pσ component on the terminal atoms. However, it is noted that the 1s$\rightarrow 8\sigma$* excitation of N_2O and 1s$\rightarrow 5\sigma_g$* excitation of CO_2 are not definitely identified as the 1s$\rightarrow 2t_2$* of CH_4. In these cases, it is reasonable to think that the valence contribution is dissolved in the Rydberg sea [1,6,12].

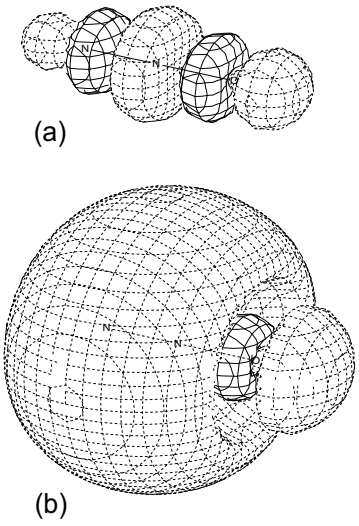

FIG. 7: Contour maps of (a) the lowest σ* (8σ*) orbital obtained without any diffuse function and (b) the RV-mixed 3sσ orbitals in the central N (N_c) 1s excitation of N_2O.

IV. SUMMARY

Using molecular orbitals, we have discussed how the 1s$\rightarrow$ σ* excited state looks like in the 1s excitation of O_2 and CH_3F, and how we know evidence for the 1s$\rightarrow$ σ* contribution in

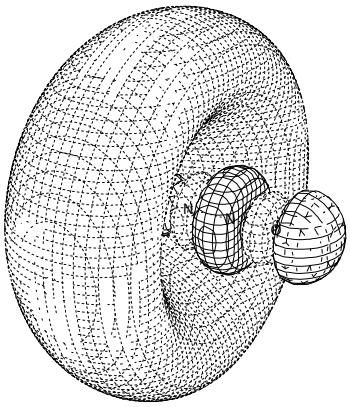

FIG. 8: A contour map of the RV-mixed 4sσ orbital in the terminal N_t 1s excitation of N_2O.

photoabsorption spectra of CH_4, CO_2, and N_2O. In the former molecules, the excitation to the σ* orbital is identified in the Franck-Condon region from the ground state; in the latter molecules, the excitation to the σ* orbital is not clearly identified but its evidence is observed through the Rydberg-valence mixing in the Franck-Condon region. In O_2, the σ* ($3\sigma_u$*) orbital is mainly mixed with the $3p\sigma_u$ Rydberg orbital converging to the $^4\Sigma^+$ ($^4\Sigma_g^+$) ionization. In CH_3F, the excitation to the σ* ($6a_1$*) orbital is observed below the $3sa_1$ Rydberg state. On the other hand, in CH_4, the Jahn-Teller distortion of the $3pt_2$ Rydberg transition induces contribution from the σ* ($2t_2$*) orbital component. In the 1s excitations from the terminal atoms in CO_2 and N_2O, some lower s-type Rydberg states get intensities from the σ* ($5\sigma_g$* and 8σ*) component. In the 1s excitations from the central atoms in CO_2 and N_2O, the 1s→ σ* excited state with *gerade-gerade* transition is a dipole-forbidden (dark) state (not exactly from N_c in N_2O). In CO_2, the C1s excitation to the $3s\sigma_g$ Rydberg orbital is vibronically enhanced through mixing with the C1s excitation to the π* ($2\pi_u$*) orbital with the Renner-Teller effect.

Acknowledgements

The author acknowledges fruitful discussion with Dr. Miyabi Hiyama from a theoretical point of view and with Dr. Jun-ichi Adachi from an experimental point of view. The present work was partly supported by Grant-in-Aid for Scientific Research (B) from the Japan Society for the Promotion of Science (JSPS).

[1] N. Kosugi, J. Electron Spectrosc. **144-147**, 1203 (2005).
[2] A. Yagishita, E. Shigemasa, and N. Kosugi, Phys. Rev. Lett. **72**, 3961 (1994).
[3] N. Kosugi, E. Shigemasa, and A. Yagishita, Chem. Phys. Lett. **190**, 481 (1992).
[4] N. Kosugi, K. Ueda, Y. Shimizu, H. Chiba, M. Okunishi, K. Ohmori, Y. Sato, and E. Shigemasa, Chem. Phys. Lett. **246**, 475 (1995).
[5] K. Ueda, M. Okunishi, H. Chiba, Y. Shimizu, K. Ohmori, Y. Sato, E. Shigemasa, and N. Kosugi, Chem. Phys. Lett. **236**, 311 (1995).
[6] M. B. Robin, *Higher Excited States of Polyatomic Molecules*, Vol. III (Academic Press, New York, 1985) p.32, p.87.
[7] N. Kosugi, in *Chemical Applications of Synchrotron Radiation*, Part I, ed. T.-K. Sham (World Scientific, Singapore, 2002). p.228.
[8] N. Kosugi, J. Electron Spectrosc. **79**, 351 (1996).
[9] J. Adachi, N. Kosugi, E. Shigemasa, and A. Yagishita, J. Phys. Chem. **100**, 19783 (1996).
[10] J. Adachi, N. Kosugi, E. Shigemasa, and A. Yagishita, J. Chem. Phys. **107**, 4919 (1997).
[11] J. Adachi, N. Kosugi, E. Shigemasa, and A. Yagishita, J. Chem. Phys. **102**, 7369 (1995).
[12] R. J. Buenker and S. D. Peyerimhoff, Chem. Phys. Lett. **36**, 415 (1975).